International Journal of Biological Macromolecules 72 (2015) 466–471

International Journal of Biological Macromolecules

journal homepage: www.elsevier.com/locate/ijbiomac

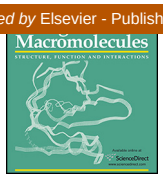

Preparation and cytotoxicity of *N*,*N*,*N*-trimethyl chitosan/alginate beads containing gold nanoparticles

Alessandro F. Martins[a,c,*], Suelen P. Facchi[c], Johny P. Monteiro[a], Samara R. Nocchi[b], Cleiser T.P. Silva[a], Celso V. Nakamura[b], Emerson M. Girotto[a], Adley F. Rubira[a], Edvani C. Muniz[a]

[a] *Grupo de Materiais Poliméricos e Compósitos, GMPC—Departamento de Química, Universidade Estadual de Maringá UEM, Av. Colombo 5790, CEP 87020-900 Maringá, Paraná, Brazil*

[b] *Laboratório de Inovação Tecnológica no Desenvolvimento de Fármacos e Cosméticos—Departamento de Ciências Básicas da Saúde, Universidade Estadual de Maringá UEM, Av. Colombo 5790, CEP 87020-900 Maringá, Paraná, Brazil*

[c] *Universidade Tecnológica Federal do Paraná (UTFPR), Estrada para Boa Esperança, CEP 85660-000 Dois Vizinhos, Paraná, Brasil*

ARTICLE INFO

Article history:
Received 3 July 2014
Received in revised form 28 July 2014
Accepted 7 August 2014
Available online 23 August 2014

Keywords:
N,*N*,*N*-trimethyl chitosan
Alginate
Beads
Polyelectrolyte complex
Gold nanoparticles

ABSTRACT

Polyelectrolyte complex beads based on *N*,*N*,*N*-trimethyl chitosan (TMC) and sodium alginate (ALG) were obtained. This biomaterial was characterised by FTIR, TGA/DTG, DSC and SEM analysis. The good properties of polyelectrolyte complex hydrogel beads were associated, for the first time, with gold nanoparticles (AuNPs). Through a straightforward methodology, AuNPs were encapsulated into the beads. The *in vitro* cytotoxicity assays on the Caco-2 colon cancer cells and healthy VERO cells showed that the beads presented good biocompatibility on both cell lines, whereas the beads loaded with gold nanoparticles (beads/AuNPs) was slightly cytotoxic on the Caco-2 and VERO cells.

1. Introduction

Chitosan (CHT) is a linear polysaccharide obtained from the deacetylation of chitin [1,2] and *N*,*N*,*N*-trimethyl chitosan (TMC) is a partially quaternised derivative of CHT that presents good solubility at a wide pH range and, therefore, overcomes the limitations in solubility presented by CHT [3–5]. Due to, mucoadhesivity, biodegradability and good antimicrobial properties of TMC, many papers focusing on this polymer have been published in the recent scientific literature reporting its biomedical applications [6–9]. Sodium alginate (ALG) is an anionic polysaccharide obtained from marine algae. ALG is a water-soluble natural copolymer composed of guluronic acid and mannuronic acid units [10]. Polyelectrolyte complexes (PECs) are made by mixing solutions of oppositely charged polyelectrolytes. The PECs-components could enable the formation of a material with controlled properties slightly [11,12].

Gold nanoparticles (AuNPs) are commonly employed as diagnostic and therapeutic agents for cancer due to their excellent biocompatibility and unique plasmonic properties [13]. AuNPs can be employed as a contrast agent for cancer detection and a therapeutic agent for cancerous cells [13,14]. Generally the surfaces of metallic nanoparticles (NPs) are charged [15,16]. Therefore, the charged surface on the NPs can bind non-specifically to biological molecules through electrostatic interactions. These interactions often result in the formation of aggregates, leading to rupture of the NPs structure [15]. The CHT and TMC have, already, been employed as stabilising agents to obtain NPs [15,17,18]. However, such cationic polymers are often dissolved in dilute acid, such as hydrochloric and acetic acid solutions. Nevertheless, AuNPs prepared using these acidic environments have limitations to biological applications due to nonspecific interactions between metallic NPs and biological tissues. The preparation of hydrogels (PECs) with loaded-AuNPs can be a strategic alternative to promote the protection of metallic NPs and also to avoid nonspecific interactions between metallic NPs and biological tissues.

Thus, the aim of this work was to prepare new polymeric hydrogel beads based on polyelectrolyte complexes (PECs) of *N*,*N*,*N*-trimethyl chitosan/alginate (TMC/ALG) and incorporate gold

* Corresponding author at: Universidade Tecnológica Federal do Paraná, Estrada para Boa Esperança, Km 04, Dois Vizinhos, Brazil.Tel.: +55 46 3536 8413; fax: +55 46 3536 8400.
E-mail address: afmartins50@yahoo.com.br (A.F. Martins).

http://dx.doi.org/10.1016/j.ijbiomac.2014.08.020
0141-8130/

nanoparticles within these beads. This paper describes, for the first time, the association of AuNPs with a system formed by a polyelectrolyte complex (PEC) of TMC/ALG. The resulting system could be used for biological applications, since the beads matrix protect the AuNPs. So, the good properties of both components (TMC and ALG), including the interesting properties of AuNPs, were combined. Additionally, the cytotoxic effects of raw beads and beads/AuNPs systems on human colon cancer cells (Caco-2 cells) and healthy cells of the African green monkey (VERO cells) were evaluated.

2. Experimental

2.1. Materials

Chitosan (CHT) with a deacetylation degree equal to 85% and M_V of 87×10^3 g mol^{-1} was purchased from Golden-Shell Biochemical (China). Sodium alginate was purchased from Across Organics (New Jersey, USA) and the ratio of mannuronic acid to guluronic acid (M/G) of the alginate was 1.56, as stated by the manufacturer. It has already been reported that the values of the average number (M_n) and average-weight (M_w) molecular weights for this alginate are 339,000 g mol^{-1} and 1073,000 g mol^{-1}, respectively [2]. Methyl iodide, *N*-methyl-2-pyrrolidinone, gold chloride(III) and sodium citrate were purchased from Sigma-Aldrich. Other reactants such as sodium hydroxide, sodium iodide, sodium chloride, sodium acetate, acetic acid, hydrochloric acid, potassium dihydrogen phosphate, ethanol and diethyl ether were also utilised in this work; all were of analytical grade. All reagents were used as received without any further purification. VERO (African green monkey kidney) cells and the Caco-2 cell line, which originated from a human colonic adenocarcinoma, were cultured and maintained in Dulbecco's modified Eagle's medium (DMEM; Gibco®, Grand Island, NY, USA) supplemented with 10% heat-inactivated foetal bovine serum (FBS; Gibco®) and 50 μg ml^{-1} gentamycin, in an incubator at 37 °C, with 5% CO_2 and 95% relative humidity. The cells were expanded when the monolayer reached confluence at day 3 ± 1. After reaching 80% confluence, cells were digested by using Trypsin/EDTA solution (0.25% trypsin—Gibco®, and 1 mmol l^{-1} EDTA).

2.2. Synthesis of N,N,N-trimethyl chitosan (TMC)

The one-step methodology employed for the synthesis of TMC is based on the method published by Martins et al. [2]. The reaction procedure used to synthesise the TMC is described in the Supplementary material.

2.3. Preparation of beads based on TMC/alginate polyelectrolyte complex

The methodology employed for the preparation of beads was based on the method published by Martins et al. [2] with some modifications. TMC and ALG solutions were prepared separately, from the solubilisation of both polymers in a 1.0% (v/v) acetic acid solution. The volume ratio of TMC-solution to ALG-solution was kept constant. The following procedure was adopted: aqueous solutions of TMC (1.0 g in 100 ml of acetic acid solution) and ALG (0.5 g in 100 ml of acetic acid solution) were prepared. The TMC-solution 1.0% (wt/v) was split into five aliquots of 20 ml. Afterwards, 5 ml of distilled water was added to 10 ml of a previously prepared ALG-solution (0.5% wt/v) and, then this diluted solution was slowly dropped into a respective TMC-solution aliquot (20 ml), at room temperature under magnetic stirring, keeping the volume ratio at 3/4 (ALG-solution/TMC-solution). The pH of the suspension containing the beads was approximately 3.5. The beads formed almost immediately. Acetone aliquots (≈5 ml) were dropped into the suspension (35 ml) containing the beads. The suspension was slowly stirred and allowed to stand for approximately 1.0 min, until complete decantation of the beads was achieved and then ≈20 ml of supernatant was removed. This process was repeated once more and the internal water content of the beads diminished substantially, leading the beads to shrivel up. Thus, the beads presented mechanical consistency and the liquid phase composed of water and acetone (≈25 ml) was easily removed from the suspension. This process prevented the beads from adhering to each other causing the collapse. Finally, the beads were washed twice with acetone, transferred to a polystyrene Petri dish and separated from each other. The drying of beads was performed at room temperature for 48 h.

2.4. Synthesis of gold nanoparticles (AuNPs)

The gold nanoparticles (AuNPs) were synthesised from the method developed by Turkevich et al. [19] with some adaptations. The methodology is described in detail in the Supplementary material.

2.5. Preparation of TMC/alginate beads loaded with gold nanoparticles (AuNPs)

Initially, AuNPs-suspension (5.0 ml containing 19.7 mg of Au^0) was added to 10 ml of a previously prepared ALG-solution (0.5% wt/v) and the mixture was stirred until homogenisation occurred. Then, the ALG-solution/AuNPs (15 ml) was slowly dropped into a respective TMC-solution aliquot (20 ml), under magnetic stirring at room temperature. Finally, the beads loaded with AuNPs (beads/AuNPs) were separated from the suspension following the same methodology as described earlier for TMC/ALG beads. It was considered that the loading efficiency of AuNPs into hydrogel beads was *ca.* 100%, since UV–vis measurements from the beads/AuNPs suspension at 518 nm no indicated the presence of the AuNPs.

2.6. Characterisation

2.6.1. Characterisation of AuNPs

The experimental procedures to characterise the AuNPs are described in the Supplementary material.

2.6.2. Characterisation of raw beads and beads loaded with metallic nanoparticles

2.6.2.1. FTIR spectroscopy. FTIR was used to characterise the chemical structure of materials (ALG, TMC and beads). In each case, KBr disc with 1.0 wt% of sample was prepared. The equipment from Shimadzu Scientific Instruments (Model 8300, Japan) was used at the following conditions: range of 4000–500 cm^{-1}, resolution of 4 cm^{-1} obtained after cumulating 64 scans.

2.6.2.2. Scanning electron microscopy (SEM). The morphology of beads and beads/AuNPs was investigated using SEM images (Shimadzu, model SS 550, Japan). Beads and beads/AuNPs surfaces were sputter-coated with a thin layer of gold for SEM visualisation. The SEM images were taken by applying an electron accelerating voltage of 15 kV.

2.6.2.3. Thermal analysis through TGA/DSC analysis. Thermalgravimetric analysis (TGA) was carried out on a thermogravimetric analyser (Netzsch, model STA 409 PG/4/G Luxx, USA) at a rate of 10 °C min^{-1} under nitrogen gas flowing at 20 ml min^{-1} in the range of 25–400 °C. DSC analyses were performed on a calorimeter (Netzsch, model STA 409 PG/4/G Luxx, USA) operating at the following conditions: heating rate of 10 °C min^{-1}, nitrogen flow rate of 50 ml min^{-1}, temperature range from 40 to 210 °C.

2.7. Cytotoxicity assays

The cytotoxicity activity of raw beads and beads/AuNPs against VERO and Caco-2 cells were determined by sulforhodamine B assay [20]. The cells were seeded in 96-well tissue plates (TPP—Techno Plastic Products, Switzerland) at a density of 2.5×10^5 (VERO cell) and 8×10^5 cell ml^{-1} (Caco-2 cell) in 100 μl medium for 24 h in the CO_2 incubator. The beads or beads/AuNPs were placed in water and were added to the medium at various concentrations after 8 h. Following incubation for 48 h, the cell monolayers were washed using 100 μl phosphate buffered saline (PBS) sterile, fixed with trichloroacetic acid and stained for 30 min with 0.4% (wt/v) sulforhodamine B (SRB-Sigma Chemical Co., St. Louis, MO, USA) dissolved in 1% acetic acid. The dye was removed by four washes with 1% acetic acid, and protein-bound dye was extracted with 10 mM unbuffered Tris base [tris (hydroxymethyl)aminomethane] for determination of optical density in a computer-interfaced, 96-well microtitre plate reader (Power Wave XS, BIO-TEK®, USA).

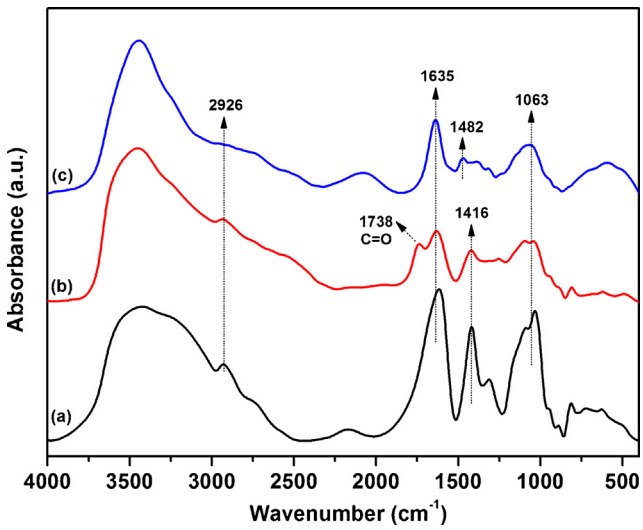

Fig. 1. FTIR spectra of ALG (a), beads (b) and TMC (c).

3. Results and discussion

3.1. Characterisation by ^1H NMR and FTIR spectroscopy

^1H NMR spectra of CHT and TMC are shown in Fig. S1 (Supplementary material). All of the signals in the ^1H NMR spectra were attributed and related to the polysaccharide structures (Scheme S1, Supplementary material). Fig. 1 shows the FTIR spectra of ALG, TMC and TMC/ALG beads. The wide band in the range from 2350 to 3710 cm^{-1} in the FTIR spectra was assigned to the characteristic stretches of C—H, N—H and O—H bonds and can be observed in all of the spectra shown in Fig. 1. On the other hand, the band at 1474 cm^{-1} (curve c) was attributed to the angular deformation of C—H bonds of N-methyl groups existing in the TMC structure [12]. The band at 1638 cm^{-1} in the FTIR spectrum of beads (curve b) was attributed to C=O bonds of secondary amide groups, referring to the acetylated residues that remain in the structure of TMC and axial asymmetric deformation of carboxylate anions [10]. The bands that appear at 1420 cm^{-1} were assigned to axial symmetric deformation of carboxylate anions [10]. This band presented a lower intensity in the beads FTIR spectrum compared to the spectrum of ALG (curve a) due to the protonation of the carboxylate anions of ALG and

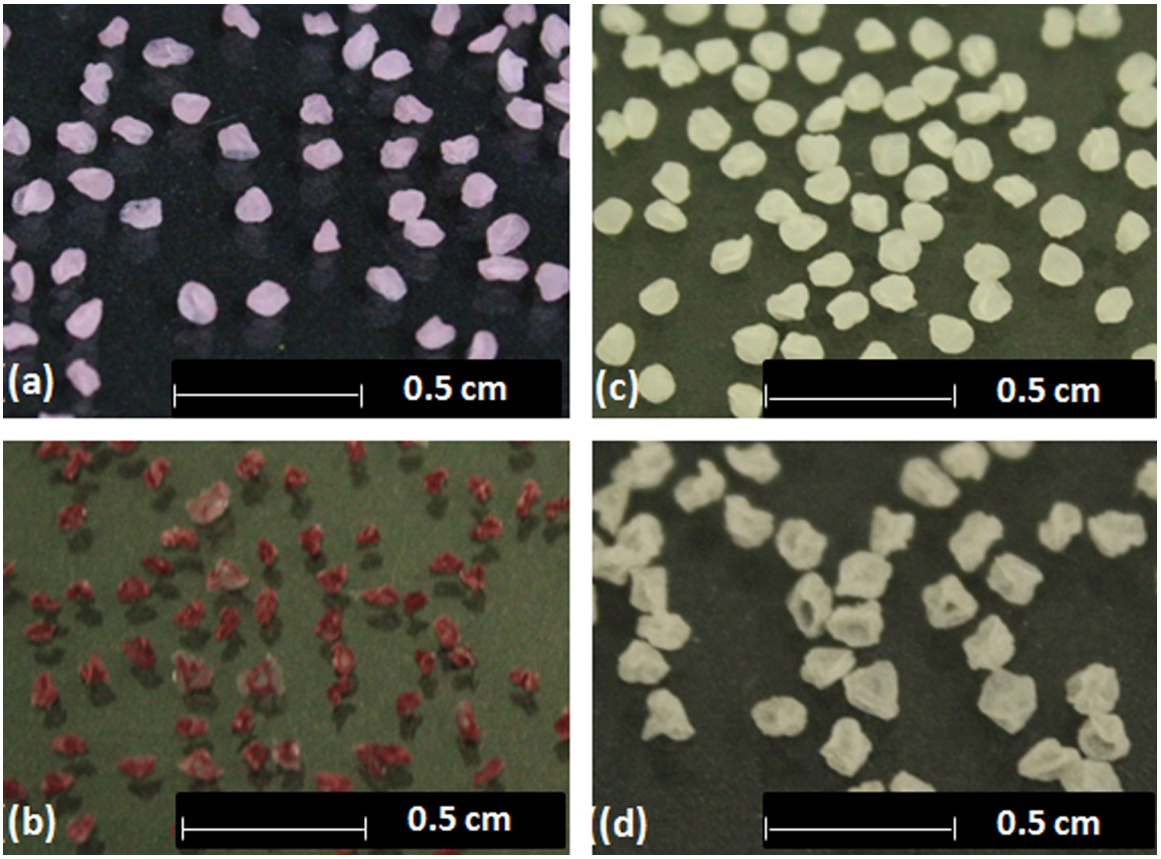

Fig. 2. Photos of beads/AuNPs (a and b) and raw beads (c and d), being the images (a and c) processed immediately after the washing with acetone and the images (b and d) obtained after some minutes (*ca.* 15 min) subsequent to the purification process.

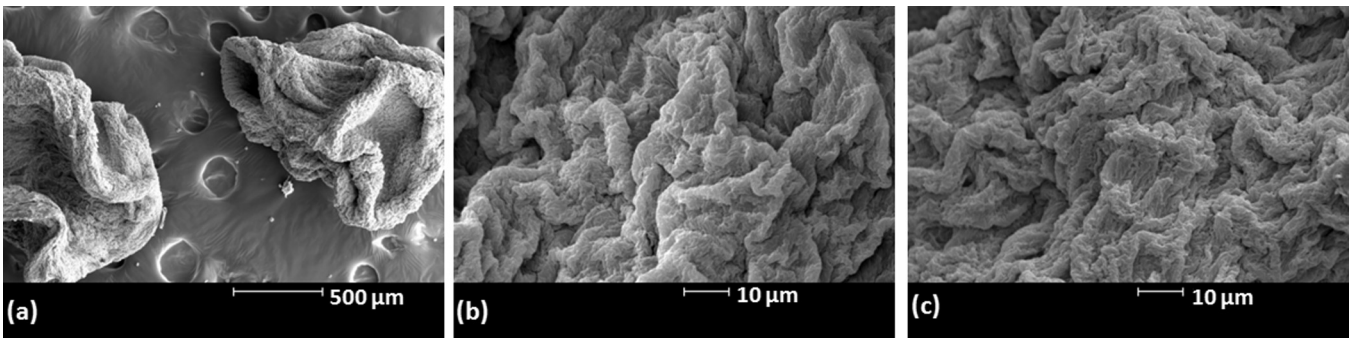

Fig. 3. SEM images of droughts samples with different magnifications: ((a and b)) raw beads and (c) beads/AuNPs.

also due to the complexation among these carboxylate anions with positively charged sites of TMC molecules.

The band at 1735 cm^{-1} on the FTIR spectrum of beads was assigned to the C=O bonds of carboxylic groups (Fig. 1). ALG is an anionic block copolymer of α-(1-4)-L-guluronic (G) and β-(1-4)-D-mannuronic acid (M). The p*K*a values of M and G-residues are 3.38 and 3.65, respectively [2]. Thus, some of the carboxyl groups of ALG remain non-ionised since the final pH of the bead suspension was approximately 3.5. Also, a broadening in the range from 2250 to 3500 cm^{-1} in FTIR spectrum of beads was verified and assigned to H-bonds among TMC-ALG in addition to the already existing interactions on TMC–TMC and ALG–ALG chain segments. The band at 1063 cm^{-1}, attributed to the stretching of C—O bonds of primary alcohols, presented noticeable differences in the FTIR spectra (Fig. 1) [12]. These differences were mainly due to associations among chain segments of ALG and TMC molecules.

3.2. Morphological analysis

Fig. S2 (Supplementary material) display the characteristic Localised Surface Plasmon Resonance (LSPR) bands of AuNPs colloidal suspensions and TEM images of AuNPs. The AuNPs size distribution were determined from Fig. S2(b). The size of AuNPs was approximately 17.6 ± 4.3 nm (Fig. S2c). The preparation and characterisation of the TMC/ALG polyelectrolyte complex is described in a paper recently published by our group [2].

Fig. 2 show images of the beads loaded with gold nanoparticles, (beads/AuNPs) and the polymeric matrix without AuNPs. The images were processed after the hydrogel purification. The beads or beads/AuNPs presented a diameter of approximately 1 to 2 mm (Fig. 2). Photos (Fig. 2) of the beads/AuNPs (a,b) and raw beads (c,d), processed immediately after washing (a,c) can be seen in Fig. 2. On the other hand, Fig. 2 (b,d) shows photographs of beads/AuNPs and raw beads obtained after a few minutes subsequent to the washing process. The colour presented by beads/AuNPs indicates the incorporation of AuNPs into the hydrogel (Fig. 2). The beads/AuNPs are reddish due to the presence of AuNPs. On the other hand, the neat TMC/ALG beads are white, as expected (Fig. 2).

Fig. 3 shows SEM images, at different magnifications, of the dry neat beads and drought beads/AuNPs. It was possible to observe "folding" on the surface of neat beads and beads/AuNPs which hindered the pores of the materials (Fig. 3). The morphologies of neat beads and beads/AuNPs are slightly differents. The AuNPs entrapped into hydrogel changes beads morphology.

3.3. Characterisation of beads by TGA/DSC analysis

TGA/DTG curves of beads and beads/AuNPs are shown in Fig. 4. Two events of mass loss were observed in the TGA curves (Fig. 4a). The first stage occurs in the range of 25 to 130 °C and was attributed to loss of water and volatile components. The second stage of mass loss was attributed to degradation of the materials, as shown in

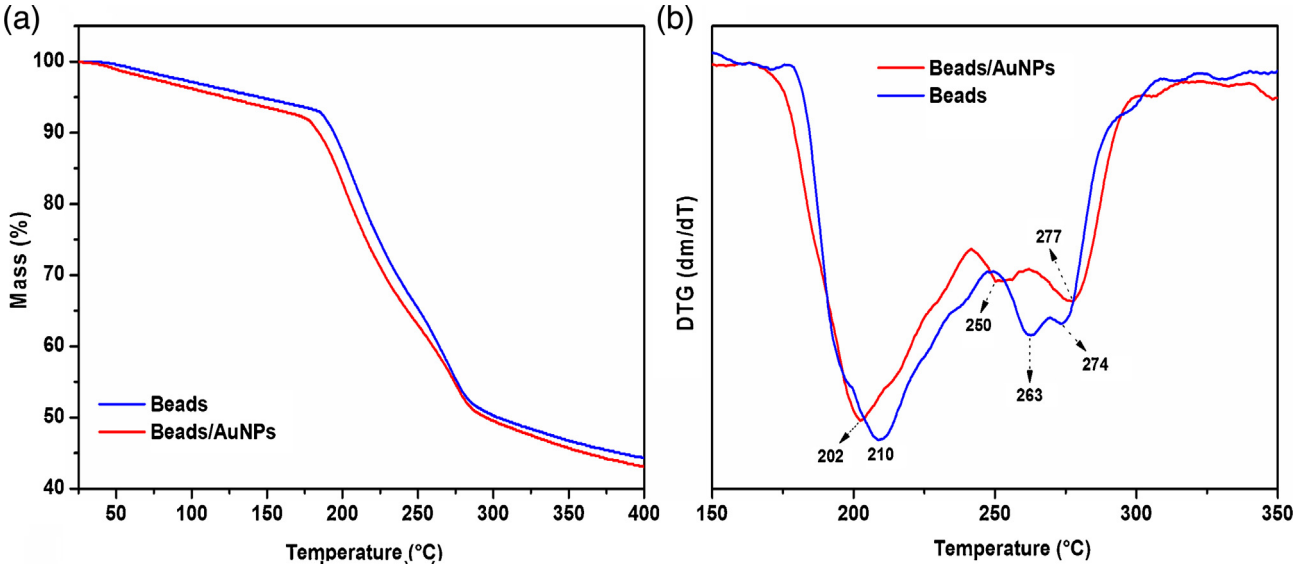

Fig. 4. TGA curves of raw beads and beads/AuNPs (a). DTG curves of raw beads and beads/AuNPs (b).

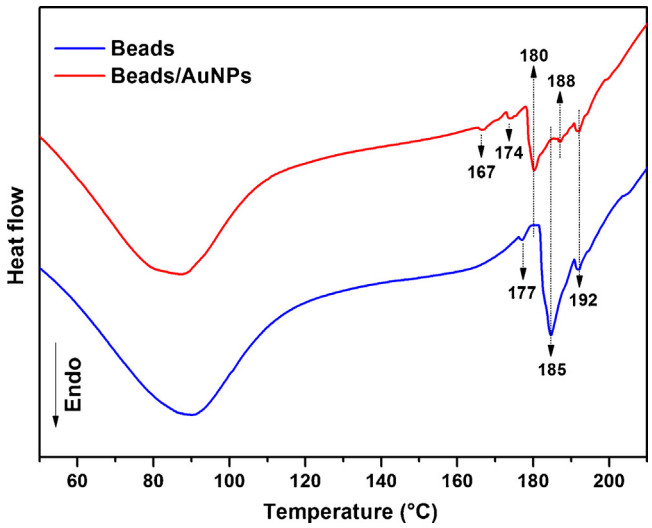

Fig. 5. DSC curves of raw beads and beads/AuNPs.

Fig. 4a in the range of 175 to 300 °C. It was observed that the beads presented high thermal stability relation to beads/AuNPs. The incorporation of AuNPs destabilised the beads, due to the increase of negative charge density in the hydrogel matrix. The effect was best seen from DTG and DSC curves of the respective materials.

The first derivatives of degradation stage (second event on TGA curves) for beads and beads/AuNPs are presented in Fig. 4b. It is possible to observe that samples presented different degradation temperatures, as indicated by the inflexion points in the DTG curves. The degradation temperatures of the beads occur at 210, 263 and 274 °C, whereas beads/AuNPs samples showed degradation temperatures at 202, 250 and 277 °C. This fact reinforces the AuNPs encapsulation.

The DSC curves of neat beads and beads/AuNPs are shown in Fig. 5. The endothermic peaks that appear in the range from 25 to 130 °C were attributed to the evaporation of adsorbed water and volatile compounds. The endothermic peaks in the range from 167 to 192 °C are related to the melting point of the materials. The DSC curves of neat beads and beads/AuNPs presented significant differences. The NPs incorporation caused changes in the chain arrangement, altering the respective DSC curves. The DSC curve of neat beads showed non-pronounced endothermic peaks at 177 and 192 °C and a more pronounced endothermic peak at 185 °C, which was the last assigned to melting of the crystalline parts of the beads.

The highest intensity endothermic peak on DSC curves of the beads/AuNPs is due to the melting that occurred at 180 °C, but this was less intense compared to neat beads. For the beads/AgNPs, such an event occurred at 188 °C but the intensity was still lower. The DSC curve of beads/AuNPs still showed no pronounced endothermic peaks at 167, 174, 188 and 192 °C. Thus, the differences in DSC curves were related to the insertion of AuNPs in the hydrogel matrix, which promoted changes in the packing of chains related to neat beads.

3.4. Cytotoxicity assays

The cytotoxic effects of beads and beads/AuNPs systems were investigated on human colon cancer cells (Caco-2 cells) and healthy VERO cells. To assess the toxicity threshold for the two different materials presented in this work, viability cell assays were conducted, using increasing concentrations of beads and beads/AuNPs for 24 h incubation periods (Fig. 6). It was verified that the beads/AuNPs were more destructive against VERO cells than against Caco-2 cancer cells (Fig. 6) when both cells-type were incubated in similar conditions. On the other hand, the formulations of neat beads showed low cytotoxicity against both cell lines studied (Fig. 6). The cytotoxicity effect of beads/AuNPs on the Caco-2 and VERO cells was evidenced due to a decrease in cell viability at concentrations above 100 μg ml^{-1} (Fig. 6). The effect induced by the presence of beads/AuNPs seems to play an opposite role with regard to the fate of cells compared with beads, being slightly less drastic for Caco-2 colon cancer cells with a viability of 80%, but slightly more destructive for healthy VERO cells, with viability decreased to 75% (Fig. 6). On the other hand, the plots reveal that raw beads

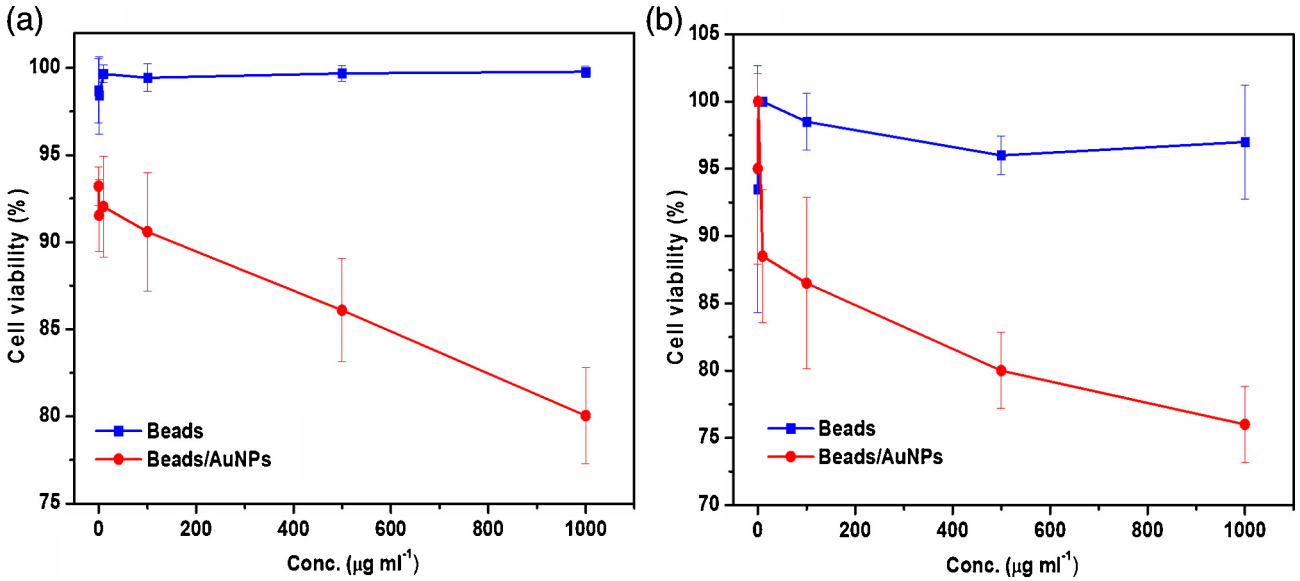

Fig. 6. Cytotoxicity effect of beads and beads/AuNPs on the viability of Caco-2 human colon cancer cells (a) and VERO healthy cells (b) at different concentrations. Error bars represent the standard deviation of two measurements.

exhibit quite good biocompatibility with healthy VERO and Caco-2 cells over the full range of concentrations as approximately 100% of the total (VERO and Caco-2) cells remained viable after 24 h of incubation.

Boca and co-workers studied the cytotoxic effect of poly (ethylene glycol)-coated with gold nanorod particles (PEG/AuNPs) on healthy human embryonic cells (HEK) and human non-small lung cancer cells (NCI-H460). According to Boca et al. [14], the PEG/AuNPs sample was biocompatible with the NCI-H460 cancer cells and had a slightly cytotoxic effect on the HEK healthy cells. Therefore, it can be stated that the beads/AuNPs prepared in this work showed different properties to the PEG/AuNPs systems studied by Boca et al. [14]. In this case, beads/AuNPs was slightly cytotoxic on the cancerous (Caco-2 cells) and healthy cells (VERO cells).

Polymeric nanocomposites based on the CHT/metallic nanoparticles were extensively studied [21–23]. As it contains functional groups in the form of amino sites, the CHT is used as a protecting agent of AuNPs and, due to the extraordinary biocompatibility and biodegradation of CHT, nanocomposites based on CHT/metallic nanoparticles have attracted much attention in the last years [15,21,24]. However, the association between TMC/ALG complex and AuNPs yet no were studied. The cytotoxic effect on both cells is related to the AuNPs and the hydrogel (beads) is useful as it can protect these NPs, inhibiting nonspecific interactions between AuNPs and biological tissues and consequently avoids aggregates formation and rupture of the AuNPs structure. UV–vis measurements showed that the AuNPs releasing no occurs from beads/AuNPs during the tests performed (not shown). The interactions among beads-AuNPs maintain the NPs stabilised in the hydrogel matrix. The AuNPs entrapped in the beads surface were responsible for the cytotoxicity shown on the Caco-2 and VERO cells.

4. Conclusions

The TMC/alginate beads showed efficiency in protecting AuNPs incorporated into the hydrogel. The cytotoxicity assays demonstrated that the neat beads exhibited excellent biocompatibility on VERO and Caco-2 cells while beads/AuNPs showed lightly cytotoxic effect against both cell lines studied. The cytotoxicity property of beads/AuNPs should be due the presence of AuNPs entrapped on the beads surface. The results presented here offer new perspectives for *in vivo* testing of the materials developed in this work.

Acknowledgments

The authors thank CNPq/CAPES, Brazil, for the doctorate fellowship (AFM) and for the financial support (Proc. 481424/2010-5 and Proc. 308337/2013-1).

Appendix A. Supplementary data

Supplementary data associated with this article can be found, in the online version, at http://dx.doi.org/10.1016/j.ijbiomac.2014.08.020.

References

[1] A.F. Martins, D.M. de Oliveira, A.G.B. Pereira, A.F. Rubira, E.C. Muniz, Int. J. Biol. Macromol. 51 (2012) 1127–1133.
[2] A.F. Martins, P.V.A. Bueno, E.A.M.S. Almeida, F.H.A. Rodrigues, A.F. Rubira, E.C. Muniz, Int. J. Biol. Macromol. 57 (2013) 174–184.
[3] S.R. Mao, X.T. Shuai, F. Unger, M. Wittmar, X.L. Xie, T. Kissel, Biomaterials 26 (2005) 6343–6356.
[4] V.K. Mourya, N.N. Inamdar, J. Mater. Sci.-Mater. Med. 20 (2009) 1057–1079.
[5] A.F. Martins, P.V.A. Bueno, H.D.M. Follmann, S.R. Nocchi, C.V. Nakamura, A.F. Rubira, E.C. Muniz, Carbohydr. Res. 381 (2013) 153–160.
[6] H. Chen, J. Wu, M. Sun, C. Guo, A. Yu, F. Cao, L. Zhao, Q. Tan, G. Zhai, J. Liposome Res. 22 (2012) 100–109.
[7] D. de Britto, M.R. de Moura, F.A. Aouada, L.H.C. Mattoso, O.B.G. Assis, Food Hydrocoll. 27 (2012) 487–493.
[8] M. Guan, Y. Zhou, Q.-L. Zhu, Y. Liu, Y.-Y. Bei, X.-N. Zhang, Q. Zhang, Nanomed.-Nanotechnol. Biol. Med. 8 (2012) 1172–1181.
[9] H. Nazar, D.G. Fatouros, S.M. van der Merwe, N. Bouropoulos, G. Avgouropoulos, J. Tsibouklis, M. Roldo, Eur. J. Pharm. Biopharm. 77 (2011) 225–232.
[10] Y.-C. Ho, F.-L. Mi, H.-W. Sung, P.-L. Kuo, Int. J. Pharm. 376 (2009) 69–75.
[11] A.F. Martins, A.G.B. Pereira, A.R. Fajardo, A.F. Rubira, E.C. Muniz, Carbohydr. Polymers 86 (2011) 1266–1272.
[12] A.F. Martins, J.F. Piai, I.T.A. Schuquel, A.F. Rubira, E.C. Muniz, Colloid Polym. Sci. 289 (2011) 1133–1144.
[13] C. Guo, J. Wang, Z. Dai, Microchim. Acta 173 (2011) 375–382.
[14] S.C. Boca, M. Potara, A.-M. Gabudean, A. Juhem, P.L. Baldeck, S. Astilean, Cancer Lett. 311 (2011) 131–140.
[15] Y. Ding, X.-H. Xia, C. Zhang, Nanotechnology 17 (2006) 4156–4162.
[16] A.D. Tiwari, A.K. Mishra, S.B. Mishra, O.A. Arotiba, B.B. Mamba, Int. J. Biol. Macromol. 48 (2011) 682–687.
[17] H.Z. Huang, X.R. Yang, Biomacromolecules 5 (2004) 2340–2346.
[18] H.H. Park, T.R. Lee, J. Nanopart. Res. 13 (2011) 2909–2918.
[19] J. Turkevich, P.C. Stevenson, J. Hillier, Discuss. Faraday Soc. 11 (1951) 55–75.
[20] P. Skehan, R. Storeng, D. Scudiero, A. Monks, J. McMahon, D. Vistica, J.T. Warren, H. Bokesch, S. Kenney, M.R. Boyd, J. Nat. Cancer Inst. 82 (1990) 1107–1112.
[21] M.J. Laudenslager, J.D. Schiffman, C.L. Schauer, Biomacromolecules 9 (2008) 2682–2685.
[22] M. Carmen Rodriguez-Argueelles, C. Sieiro, R. Cao, L. Nasi, J. Colloid Interface Sci. 364 (2011) 80–84.
[23] T. Hoang Vinh, T. Lam Dai, B. Cham Thi, V. Hoang Dinh, N. Thinh Ngoc, P. Dien Gia, N. Phuc Xuan, Colloids Surf., A: Physicochem. Eng. Aspects 360 (2010) 32–40.
[24] P. Jena, S. Mohanty, R. Mallick, B. Jacob, A. Sonawane, Int. J. Nanomed. 7 (2012) 1805–1818.